Robustness Comparison of Synthetic Inertia Strategies for Doubly Fed Induction Generators under Different Operating Conditions

Paulo Andrade Souza, *
Renan R. dos Santos, Manoelito C. N. Filho, Daniel Barbosa, **
Luciano Sales Barros ***

* UNIFACS/UFBA (e-mail: paulo.andrade@unifacs.br).
** UFBA (e-mail: renanrodrigues11@hotmail.com,
manoelitofilho@gmail.com, dbarbosa@ufba.br)
*** UFPB, (e-mail: lsalesbarros@gmail.com)

Abstract:
Due to the increasing penetration of Renewable Energy Sources (RES) such as wind energy in electrical grids, Wind Energy Conversion Systems (WECS) participation in primary control is becoming required including the Doubly Fed Induction Generator (DFIG)-based WECS. High integration of large scale DFIG-based WECS brings new challenges to their primary control support, and more strongly due to the wind condition and grid parameter uncertainties. One of the most used types of control strategy for DFIG-based WECS primary support is the synthetic inertia, however, robustness of these techniques have not been tested. In this work three synthetic inertia control strategies will be tested under different operating conditions of wind speed, frequency and voltage sag. For testing the DFIG-based WECS, it was modeled on ATP including its control systems and the results quantified the controllers robustness on the tested controllers with respect to transient frequency behavior.

Keywords: Synthetic Inertia, DFIG, ATP, Primary Control Support, Wind Power

1. INTRODUCTION

Renewable energy sources have become increasingly important for the development of electric power systems, making a significant contribution to power generation worldwide. As its use grows, the need of detailed analysis to ensure the correct operation of Electrical Power Systems (EPS) also increases(Marinescu and Serban, 2009).

Extensive studies have been performed by the Electric Power System (EPS) Operators to implement actions to combat the reduction of the general inertia due to the increased penetration of wind generation. The available Synthetic Inertia strategies can be divided into two main families: WECS Concealed Energy Utilization and Stored Energy utilization. The former is characterized by the use of inertia through the existing energy in the WECS components, while the latter provides a constant contribution of energy over a period of time from a storage source. In its classic implementation, the Synthetic Inertia system provides a power contribution proportional to the frequency offset (Bonfiglio et al., 2019).

The EPS requirements currently existing and most of the proposed new ones are often vague in defining the exact terms for the provision of synthetic inertia. This can lead to unwanted disconnection of WECS, which contradicts the interest of network operators that synthetic inertia is actually supplied when necessary to ensure the improvement on EPS power quality. As wind penetration increases and when EPS inertia further decreases, synthetic inertia will need to be reliably provided by WECS at all operational points (Gloe et al., 2019).

In DFIG-based WECS, the generator stator is connected directly to the grid and the rotor is connected to the grid through two power electronics converters and a DC link (Elmouhi et al., 2019).

It is known that low inertia can cause high frequency gradients due to unbalances between generation and load during and after disturbances and therefore increases the risk of safe violations of the power system frequency operating limits (Canevese et al., 2017). Synthetic inertia control has been proposed and developed by several authors (Bonfiglio et al., 2019; Taczi, 2017; Chamorro et al., 2017a; Liu and Lindemann, 2018; Dharmawardena et al., 2016; Bignucolo et al., 2019), showing improvements in the frequency stability of the network. However, the robustness analysis of these works' proposed controllers still need to be expanded.

The effectiveness of using synthetic inertia by controlling the machine's operation point of the active power and torque from frequency variations has already been demonstrated by other authors. However, its application in real systems, the quantification of their contributions, the analysis of storage energy need, the robustness quan-

tification of the controllers and the improvement of norms and standards still need to be better studied.

Detailed dynamic EPS simulations are known to be required to analyze the actual impacts on system stability using WECS synthetic inertia. These simulations involve frequency stability analyzes of system behavior after grid disturbances, such as sudden disconnects from generators or loads. These robustness simulations require modeling of Maximum Power Point Tracking (MPPT) and synthetic inertia control structures (Cieslak and Grunwald, 2019).

In this article, three control strategies of synthetic inertia control will be tested for DFIG-based WECS under different operating conditions: wind speeds, under frequency and voltage sags. For testing the DFIG-based WECS, it was modeled on ATP, including its control systems, and the results quantified the robustness of the tested Controllers to transient frequency behavior.

This work aims to contribute to the study of synthetic inertia by analyzing the robustness of three distinct control strategies in the face of variations in operating conditions of a real system.

This work is divided into six sections besides the bibliographic reference. Section II and III detail the control strategies, section IV detail the systems and sections V and VI presents the results and considerations.

2. SYNTHETIC INERTIA CONTROL STRATEGIES

With the rapid wind energy penetration increase in the EPS, the revision of the grid's operational requirements on frequency stability should be carried out to ensure safe and stable operation of the grid. The use of synthetic inertia in WECS is for the purpose of extracting stored inertial energy from the moving part and the link CC to provide incremental energy similar to that provided by a real inertial synchronous generator (Gao and Preece, 2017).

However, since the frequency variation depends on the active power variation and the moment of inertia observed in the electrical system, in order to provide frequency support the WECS active power injected by wind generation must increase or decrease according to the frequency variation, mode F, or according to the active power error and triggered by a frequency signal, mode P (Elmore, 2003). Thus, to respond to low frequency grid situations, the control system must allow the wind turbine to further inject the mechanical power of the wind turbine.

Frequency control must act dynamically on continuous and relatively small imbalances between generation and load, due to the impossibility of accurately anticipating their previous behavior (Elmore, 2003).

The operation of the inertia control can be observed in Fig. 1-3 where $Error\_P$ is the active power error considering the measured output power and the reference output power, $Error\_F$ is the frequency error considering the measured and the rated stator frequencies. There are two types of controller: a proportional-integral (PI) and a proportional-integral-derivative (PID). The derivative strategy, in the last one (PID), is commonly used to get fast actions from variations of signals like frequency.

Also, the DFIG Rotor Side Converter (RSC) is shown in Fig. 1-3. Finally, in Fig. 1-3, I_{rq} is the rotor current, I_{rq}^* is the desired value of the I_{rq} and V_{rq}^* is the desired value of V_{rq} for the converters.

Three tests were conducted changing the minimum frequency deviation (0.05 Hz, 0.025 Hz and 0.1 Hz) for which the synthetic inertia controller starts acting, and 0.05 Hz was the value that yielded the best results for the frequency response of the system.

These three variations are usual start-points for these types of frequency controllers (Chamorro et al., 2017b). The start-point is very important, especially for the minimum value of frequency reached during the transient period (NADIR), because anticipating the controller action usually helps the decrease of this error.

For the two first strategies the MPPT control is deactivated and the synthetic inertia is activated. In the first strategy (Power Error Controller) shown in Fig. 1 this actuation occurs using the Power error as input. In the second strategy (Frequency Error Controller), Fig. 2, the frequency error was used as the control input so that it was possible to obtain zero error in frequency. In the third strategy (Power and Frequency Error Controller), Fig. 3, two parallel controllers were implemented, the first being the MPPT.

For all strategies, the main concern for WECS synthetic inertia emulation is system frequency measurement noise as the performance of the synthetic inertia controller can be measured by the ROCOF. In addition, the stored kinetic energy of WECS cannot be over-extracted to avoid blocking the turbine rotor (Gao and Preece, 2017).
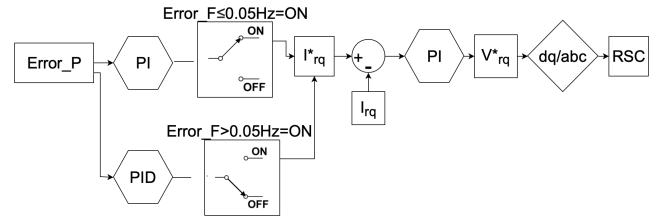
Figure 1. Power Error Controller Loop Block Diagram.
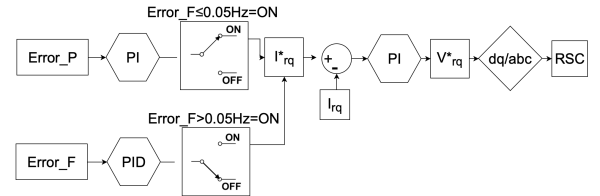
Figure 2. Frequency Error Controller Loop Block Diagram.

3. CONTROL DESIGN

The dynamic performance analysis was performed on ATP with the simulation of a real system, which allows a more detailed view of the impacts on the EPS due to variations in the scenarios. Those variations were made around a base case consisting of the operating conditions under which the controllers were tuned.
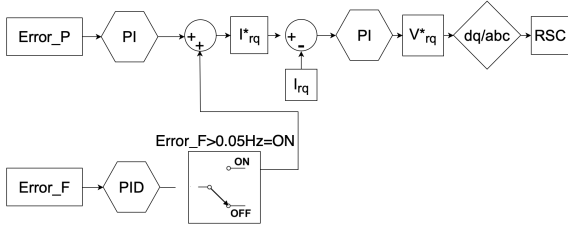
Figure 3. Power and Frequency Controller Loop Block Diagram.

The following inputs and EPS variations were simulated: equivalent network impedance variations, incident wind speed variations and short circuit impedance variations. The EPS was studied under three-phase short circuit in the PCC (Point of Common Coupling) and grid frequency and characteristics were analyzed. For these scenarios, measurements were made of the WECS main grid and the network that allowed the behavior analysis and the graphs presented in this paper.

These inputs variations were made to simulate variations on network loads and WECS operating conditions. After that, a combined variations set were made to understand the multi-variations behavior.

In order to analyze the performance of each control strategy for different PID gains, a Python (Python, 2019) platform was developed to perform a large number of simulations and minimize an objective function through heuristic methods. Other authors have had success with this methodology as seen in Xu et al. (2018); Sterling and Tyler (2018).

For controllers' tuning, based on a objective function, initially simulations were performed with incremental variations of 500 for each of the control parameters: K_p, K_i and K_d. The maximum and minimum possible gain range were 30,000 and -30,000 respectively. After this, new simulations were performed with incremental gain variations of 50 for each of the control parameters and, finally, with each of 5. A total of 2,100 simulations were performed for optimal tuning of the controllers and the gains obtained can be seen in Table 1. For the control strategies implemented, an additional active power injection was made when the system reached a frequency variation greater than 0.05 Hz.

Table 1. Frequency Controller's Gains.

Gain	Power Error Controller	Frequency Error Controller	Power and Frequency Error Controller
K_p	2550	-15.000	10
K_d	10	1.500	5.500
K_i	10	-12.000	5

4. SYSTEM CHARACTERISTIC

The development of this work is based on computational simulations using the ATP software, using a wind farm whose characteristics were obtained from a real system located in a region of high wind potential in the state of Bahia, northeast of Brazil. The WECS under analysis was interconnected to the National Interconnected System (SIN) through a 69 kV Transmission Line (LT), as shown in Fig. 4 and the system data are in Table 2.
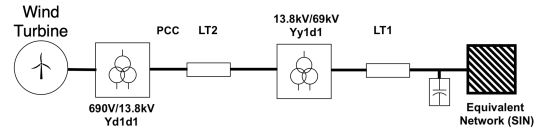
Figure 4. Single Line Electrical Diagram.

Table 2. Connection data.

SE BAHIA: $I_{sc_{3\phi}}$	$11.74\angle 89.05\ kA$
X/R Three phase	60.03
Irecê Substation: $I_{sc_{1\phi}}$	$12.28\angle 84.19\ kA$
X/R Mono phase	59.89
Conductor Diameter	$14.3\ mm$
AC Maximum Electrical Resistance	$0.26\ \Omega/km$
Inductive Reactance	$0.3925\ \Omega/km$
Capacitive Reactance	$0.2358\ \Omega.km$
Capacitive Reactive Power	$24.78\ MVAr$

The EPS analyzed contains 113 km transmission line between the Point of Common Coupling (PCC) and the base network, including the 40 MVA single-phase transformer bank of the connecting substation. The lines were modeled using the Bergeron Model using the ATP's LCC (Lines&Cables) tool. Additionally, in the PCC, a 20 MVA load was inserted in order to represent all current loads connected in the study system.

The WECS topology chosen to perform the simulations was DFIG, because it is one of the most widely used turbines in the world and in Brazil (REN21, 2019). A diagram of this connection can be seen in Fig. 5.
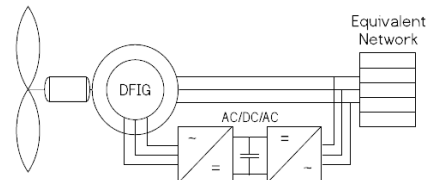
Figure 5. DFIG Wind Turbine.

The parameters of WECS modeled in ATP can be seen in Table 3.

5. RESULTS AND DISCUSSIONS

WECS rated behavior can be observed in Fig. 6 where the main outputs such as voltages and powers can be seen. Especially the synthetic inertia performance over the power grid frequency can be observed with a 50% voltage sag at PCC, during 8 to 10 s interval. Firstly, simulations were conducted varying individually the wind speed, the equivalent impedance and the short-circuit impedance. Finally, these parameters were altered simultaneously to evaluate the Controllers robustness. The presented results compare the wind turbine behavior with and without the insertion of the synthetic inertia control. The Integral Absolute Error (IAE) of frequency for the base cases of each Controller can be seen in Table 5.

In Figure 7, it presents results for variations simulated over the base case to analyze the WECS Controllers robustness.
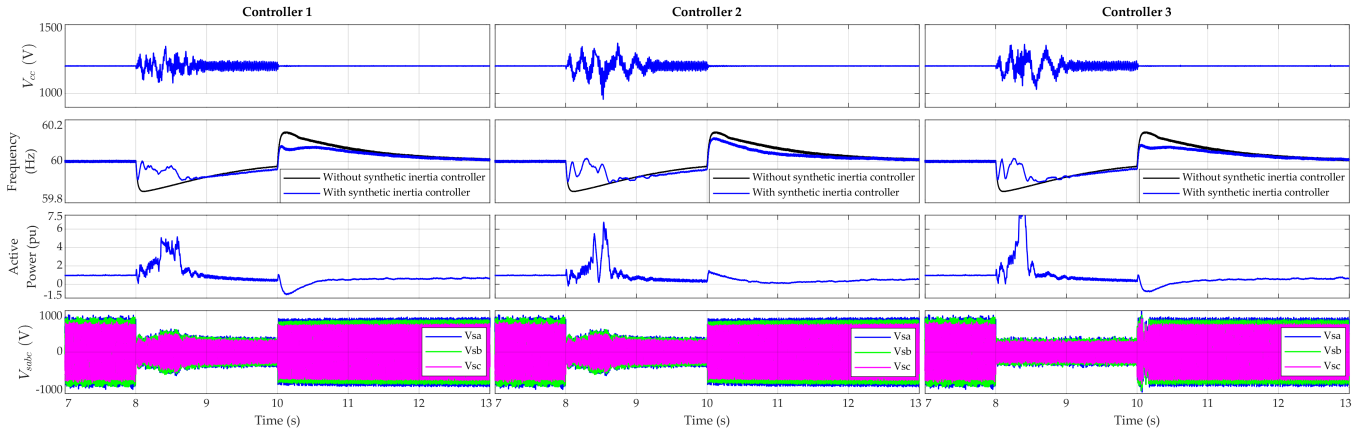
Figure 6. Sythetic Intertia Controllers.
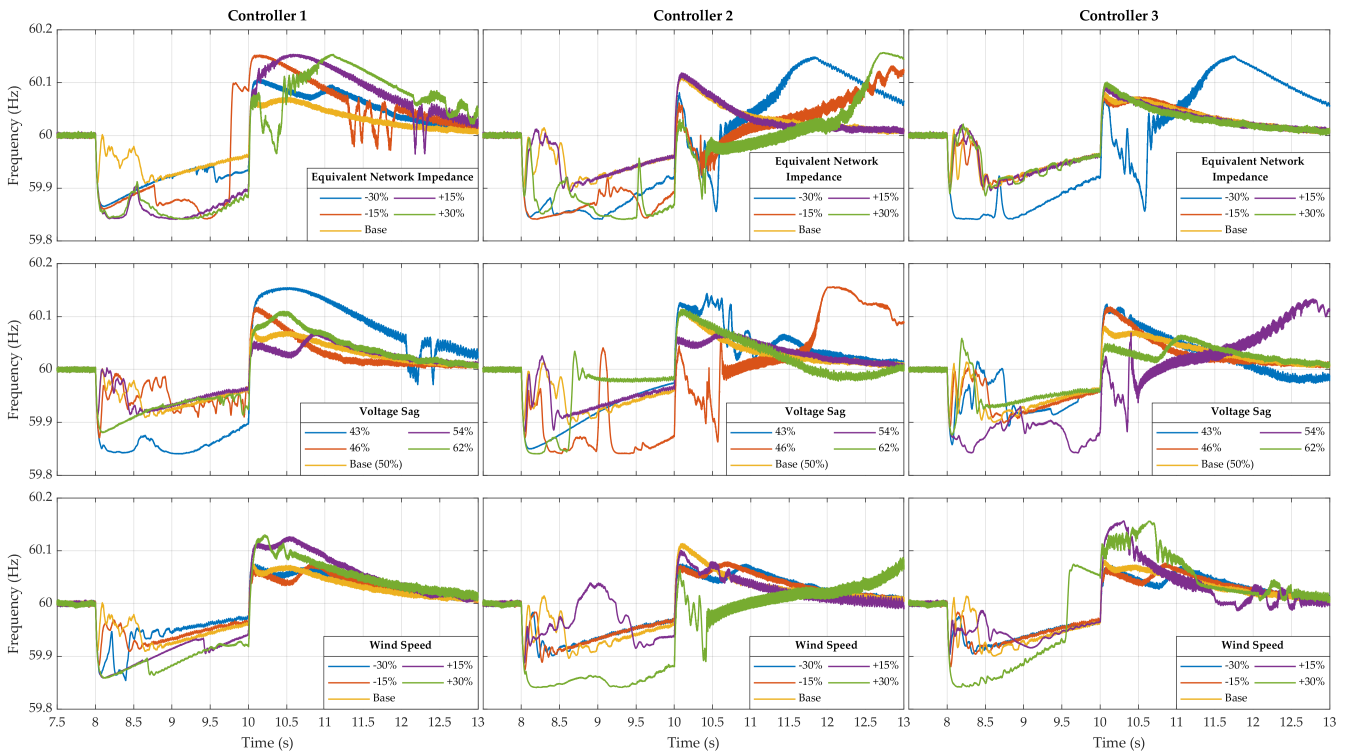
Figure 7. Variations of Operational Conditions.

Variations were made using typical occurrence values for the studied EPS to represent real changes in operating conditions such as variations in wind speed, variations in the network equivalent as a way to represent different system loads and variations in short circuit impedance to represent different voltage sags.

For the wind speed variation tests, changes of −15% for Power Error Controller, +15% for Frequency Error Controller and ±15% and −30% for Power and Frequency Error Controller did not yield an increase over 5% in the IAE compared to the base case. For all other wind speed variations, this increase exceeded 5% and the worst performance case was -30% for Frequency Error Controller, which had a 52.30% increase in the frequency IAE from the base case.

For the voltage sag severity variation tests on Power Error Controller all cases except for 43% showed good performance results, with even lower IAE compared to the base case. Only the 43% case had bad performance values with a 55.67% increase in the frequency IAE in comparison to the base case. For Frequency Error Controller, the scenarios with higher voltage sags performed well with increases in IAE under 5% from base case and the ones with lower voltage sags showed under performance with a maximum increase of 48.90% in IAE. For Power and Frequency Error Controller, just the 62% case had a better performance in comparison to the base case with a decrease in IAE of 3.88%.

For the network equivalent impedance variation tests on Power Error Controller, none of the cases were better than the base one and the minimum and maximum IAE increases from base case were 20.19% and 56.30% for -30%
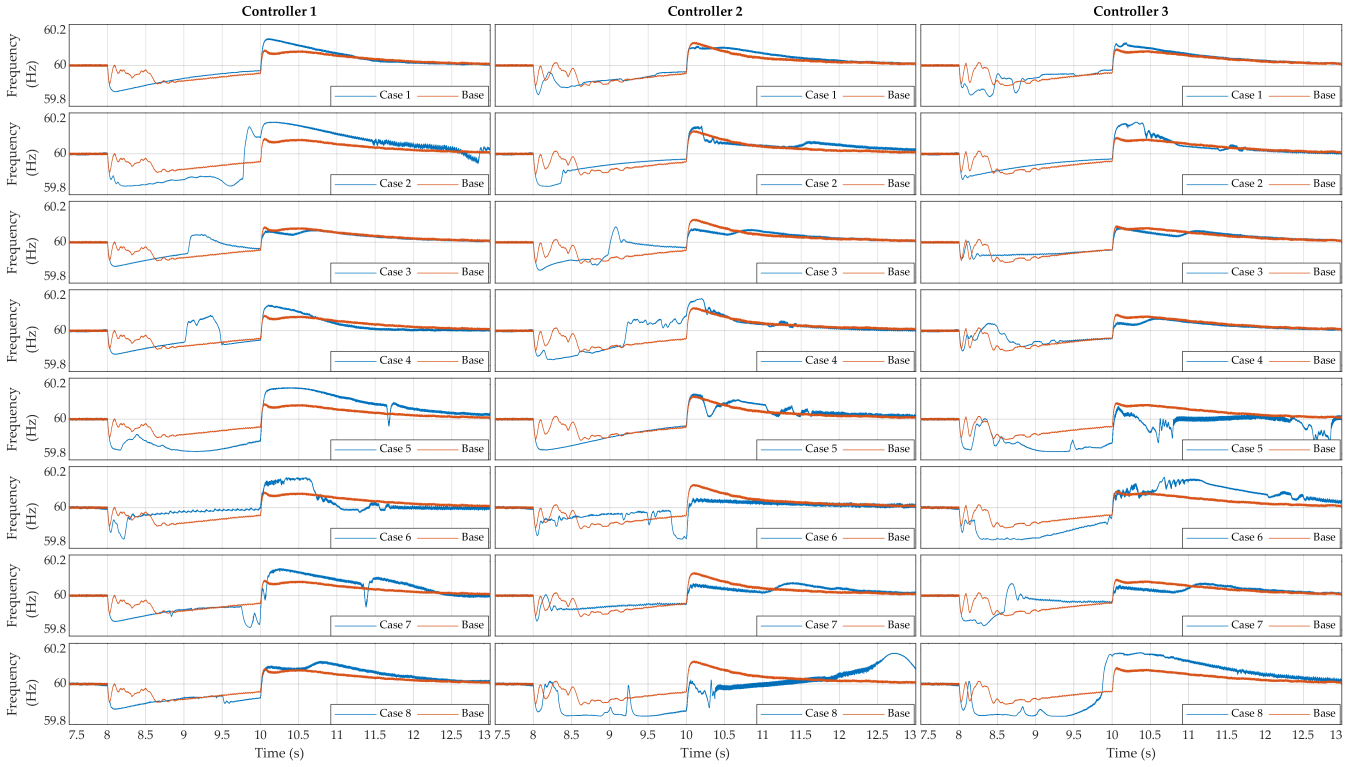
Figure 8. Combinative Variations of Operational Conditions.

Table 3. Wind Turbine Characteristics.

Characteristics	Value
Rated Power	$2\ MW$
Rated Voltage	$690\ V$
Rated Frequency	$60\ Hz$
Stator Resistance	$0.002381\ \Omega$
Stator Inductance	$1.9576\ mH$
Rotoric Resistance	$0.002381\ \Omega$
Rotoric Inductance	$1.9448\ mH$
Mutual Inductance	$1.8944\ mH$
Pairs of Poles	2
Moment of Inertia	$59\ kgm^2$
Inertia Constant	$0.52\ s$
Rotor Speed	$9-21\ rpm$
Rotor Diameter	$75\ m$
Transmission Ratio	111.5
Total Inertia Moment	$5.9 \cdot 10^6\ kgm^2$
Wind "cut-in" Speed	$4\ m/s$
Rated Wind Speed	$12\ m/s$
Wind "cut-out" Speed	$25\ m/s$
Ar Density	$1.225\ kg/m^3$
Best Espec. Speed	6.86
Max. C_p	0.42
Inertia Constant (H_t)	$4.2\ s$

Table 4. Operation Conditions Comparative to Base Case.

Cases	Equivalent Network Impedance	Voltage Sag	Incident Wind Speed
1	-30%	62%	-30%
2	-30%	62%	+30%
3	-30%	43%	-30%
4	-30%	43%	+30%
5	+30%	62%	-30%
6	+30%	62%	+30%
7	+30%	43%	-30%
8	+30%	43%	+30%

Table 5. Base Cases Frequency IAE.

Controller Error Type	Power	Frequency	Power and Frequency
Base Case IAE	$6.34\ Hz$	$6.42\ Hz$	$6.43\ Hz$

and +15% cases. For Frequency Error Controller, just the +15% case was slightly better than the base case with a decrease on IAE of 0.46% and for Power and Frequency Error Controller all cases except the −30% had similar performance with an increase of IAE under 5%. The −30% case for the Power and Frequency Error Controller had an increase of 53.49% in IAE.

The controllers were tuned under the base case operational conditions and even with fluctuations in these conditions the system did not diverge or showed behaviors that

compromised the EPS. However, it can be observed that for some operating conditions the controllers performed well and for others there were large impacts on their performances with IAE increases over 50% from base case.

The combined variations, which were made over the base case to check the influence of cumulative variations on the system performance, are shown in Fig. 8. Table 4 shows the list of cases and the operation condition variations. Similarly to individual tests the combined cases showed that the system did not diverge in any case but most of them had worse performance than the base case.

Power Error Controller case 5 was the worst case with an increase in IAE from base case of 50.31% and the best case was the case 6 with a decrease in IAE from

base case of 6.15%. The average increase in IAE from base case for Power Error Controller was 17.50%. For Frequency Error Controller case 8 was the worst case with a increase in IAE from base case of 40.03% and the best case was the case 6 with a decrease in IAE from base case of 8.58%. The average increase in IAE from base case for the Frequency Error Controller was 9.81%. For Power and Frequency Error Controller case 8 was the worst case with a increase in IAE error from base case of 46.50% and the best case was the case 4 with a decrease in IAE from base case of 8.08%. The average increase in IAE from base case for the Power and Error Controller was 13.68%. The Frequency Error Controller was more stable under operational conditions variations and the Power Error Controller was the least stable one.

6. FINAL CONSIDERATIONS

This work studied the use of synthetic inertia in DFIG-based Wind Energy Conversion Systems using the software ATP from the modeling of the connection of a 2 MW unit to an existing Electric Power System in the state of Bahia.

Even with fluctuations in the base case operational conditions the system did not diverge or show behaviors that compromised the EPS. Similarly to individual tests the combined cases showed that the system did not diverge in any case.

It was observed that the implemented controls had in some cases performance drops over 50% in Integral Absolute Error compared to the base case with the changes of the operating conditions of the system. Frequency Error Controller was more stable under operational conditions variations and the Power Error Controller was the least stable.

For future works, it is observed that a robust control strategy could be interesting in order to add robustness.

REFERENCES

Bignucolo, F., Cervi, A., and Stecca, R. (2019). Network frequency regulation with dfig wind turbines compliant with italian standards. In *2019 IEEE International Conference on Environment and Electrical Engineering and 2019 IEEE Industrial and Commercial Power Systems Europe (EEEIC / I CPS Europe)*, 1–6. doi:10.1109/EEEIC.2019.8783580.

Bonfiglio, A., Invernizzi, M., Labella, A., and Procopio, R. (2019). Design and implementation of a variable synthetic inertia controller for wind turbine generators. *IEEE Transactions on Power Systems*, 34(1), 754–764. doi:10.1109/TPWRS.2018.2865958.

Canevese, S., Iaria, A., and Rapizza, M. (2017). Impact of fast primary regulation and synthetic inertia on grid frequency control. In *2017 IEEE PES Innovative Smart Grid Technologies Conference Europe (ISGT-Europe)*, 1–6. doi:10.1109/ISGTEurope.2017.8260147.

Chamorro, H.R., Sanchez, A.C., Øverjordet, A., Jimenez, F., Gonzalez-Longatt, F., and Sood, V.K. (2017a). Distributed synthetic inertia control in power systems. In *Proc. Int. Conf. ENERGY and ENVIRONMENT (CIEM)*, 74–78. doi:10.1109/CIEM.2017.8120874.

Chamorro, H.R., Sanchez, A.C., Øverjordet, A., Jimenez, F., Gonzalez-Longatt, F., and Sood, V.K. (2017b). Distributed synthetic inertia control in power systems. In *2017 International Conference on ENERGY and ENVIRONMENT (CIEM)*, 74–78. doi:10.1109/CIEM.2017.8120874.

Cieslak, C. and Grunwald, L. (2019). Modelling synthetic inertia of wind turbines for dynamic power system stability studies. In *2019 54th International Universities Power Engineering Conference (UPEC)*, 1–6. doi:10.1109/UPEC.2019.8893593.

Dharmawardena, H., Uhlen, K., and Gjerde, S.S. (2016). Modelling wind farm with synthetic inertia for power system dynamic studies. In *Proc. IEEE Int. Energy Conf. (ENERGYCON)*, 1–6. doi:10.1109/ENERGYCON.2016.7514098.

Elmore, W.A. (2003). *Protective relaying: theory and applications*, volume 1. CRC press.

Elmouhi, N., Essadki, A., Elaimani, H., and Chakib, R. (2019). Evaluation of the inertial response of variable speed wind turbines based on dfig using backstepping for a frequency control. In *2019 International Conference on Wireless Technologies, Embedded and Intelligent Systems (WITS)*, 1–6. doi:10.1109/WITS.2019.8723766.

Gao, Q. and Preece, R. (2017). Improving frequency stability in low inertia power systems using synthetic inertia from wind turbines. In *Proc. IEEE Manchester PowerTech*, 1–6. doi:10.1109/PTC.2017.7980836.

Gloe, A., Jauch, C., Craciun, B., and Winkelmann, J. (2019). Continuous provision of synthetic inertia with wind turbines: implications for the wind turbine and for the grid. *IET Renewable Power Generation*, 13(5), 668–675. doi:10.1049/iet-rpg.2018.5263.

Liu, X. and Lindemann, A. (2018). Control of VSC-HVDC connected offshore windfarms for providing synthetic inertia. *IEEE Journal of Emerging and Selected Topics in Power Electronics*, 6(3), 1407–1417. doi:10.1109/JESTPE.2017.2751541.

Marinescu, C. and Serban, I. (2009). Analysis of frequency stability in a residential autonomous microgrid based on a wind turbine and a microhydro power plant. In *2009 IEEE Power Electronics and Machines in Wind Applications*, 1–5. doi:10.1109/PEMWA.2009.5208400.

Python (2019). Python software foundation. URL https://www.python.org. https://www.python.org.

REN21 (2019). Renewables 2018 global status report. URL http://www.ren21.net/. http://www.ren21.net/.

Sterling, G. and Tyler, B. (2018). Renewable energy management using action dependent heuristic dynamic programming. In *2018 IEEE International Smart Cities Conference (ISC2)*, 1–5. doi:10.1109/ISC2.2018.8656942.

Taczi, I. (2017). Enhancing power system frequency stability with synthetic inertia. In *Proc. IEEE EUROCON 2017 -17th Int. Conf. Smart Technologies*, 960–965. doi:10.1109/EUROCON.2017.8011254.

Xu, Y., Li, C., Wang, Z., Zhang, N., and Peng, B. (2018). Load frequency control of a novel renewable energy integrated micro-grid containing pumped hydropower energy storage. *IEEE Access*, 6, 29067–29077. doi:10.1109/ACCESS.2018.2826015.